Marfan and Loeys-Dietz aortic phenotype: A potential tool for diagnosis and management

Luigi Lovato, MD,[a] Mariano Cefarelli, MD, PhD,[b] Luca Di Marco, MD, PhD,[c] Daniel Arcioni, MD,[d] Giada Tortora, MD, PhD,[e] Ada Dormi, Mth D Biostatistical,[f] Nicolò Schicchi, MD,[g] Elisabetta Mariucci, MD, PhD,[h] Marco Di Eusanio, MD, PhD,[b] Davide Pacini, MD, PhD,[c] and Rossella Fattori, MD, PhD[i]

ABSTRACT

Objective: In heritable aortic diseases, different vascular involvement may occur with potential variable implications in aortic dilation/dissection risk. This study aimed to analyze the aortic anatomy of individuals with Marfan syndrome and Loeys-Dietz syndrome to identify possible morphological differences.

Methods: Computed tomography and magnetic resonance imaging of the thoracoabdominal aorta from the proximal supra-aortic vessels to the femoral bifurcation level of 114 patients with Marfan and Loeys-Dietz syndromes and 20 matched control subjects were examined. Aortic diameters, areas, length, and tortuosity were measured in different aortic segments using specific vessel analysis software.

Results: Patients with Marfan syndrome showed a higher prevalence of ascending aorta and aortic root dilation ($P = .011$), larger and longer aortic roots ($P = .013$) with pear-shaped phenotype, larger isthmus/descending aorta diameter ratio ($P = .015$), and larger suprarenal aorta and iliac arteries. Patients with Loeys-Dietz syndrome showed longer indexed segments and a significantly longer arch ($P = .006$) with type 2/3 arch prevalence ($P = .097$). Measurement ratios analysis provided cut-off values (aortic root to ascending aorta length/aortic root diameter, aortic root/sinotubular junction, aortic root/ascending aorta diameter) differentiating patients with Marfan syndrome from patients with Loeys-Dietz syndrome, even in the early stage of the disease.

Conclusions: Both syndromes show peculiar anatomic patterns at different aortic levels irrespective of aortic dilation and disease severity. These features may represent the expression of different genetic mutations on aortic development, with a potential impact on prognosis and possibly contributing to better management of the diseases. The systematic adoption of whole body imaging with magnetic resonance or computed tomography should always be considered, because they allow a complete vascular assessment with practical indicators of differential diagnosis. (JTCVS Open 2024;19:223-40)

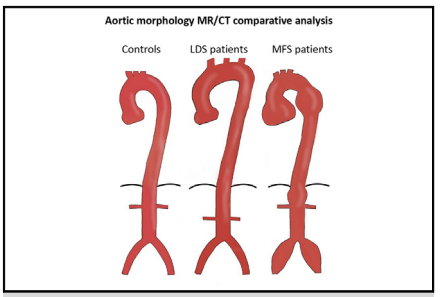

Computed tomography and magnetic resonance imaging morphologic comparison identifies aortic phenotypes for early differentiation.

CENTRAL MESSAGE

Distinct aortic patterns identified by whole-body imaging help to differentiate patients with MFS from patients with LDS, aiding early diagnosis, with a potential impact on prognosis and management.

PERSPECTIVE

Recognizing unique aortic patterns through computed tomography and magnetic resonance imaging in MFS and LDS is pivotal, shedding light on genetic influences on aortic development. A focused follow-up might be able to identify which subtype of anatomy is associated with a high risk of dissection irrespective of aortic dilation.

From the [a]Pediatric and Adult Cardiothoracic and Vascular, Oncohematologic and Emergency Radiology Unit, IRCCS Azienda Ospedaliero-Universitaria di Bologna, Bologna, Italy; [b]Cardiac Surgery Unit and Marfan Center, Lancisi Cardiovascular Center, Polytechnic University of Marche, Ancona, Italy; [c]Cardiac Surgery Unit, IRCCS Azienda Ospedaliero-Universitaria di Bologna, Bologna, Italy; [d]Fondazione Policlinico Universitario Agostino Gemelli, IRCCS-Università Cattolica del Sacro Cuore, Roma, Italy; [e]Medical Genetic Unit, Azienda Ospedaliero-Universitaria delle Marche, Ancona, Italy; [f]Department of Medical and Surgical Sciences, Alma Mater Studiorum University of Bologna, Bologna, Italy; [g]Cardiovascular Radiology Unit, Department of Radiology, Azienda Ospedaliero-Universitaria delle Marche, Ancona, Italy; [h]Pediatric Cardiology and Adult Congenital Heart Disease Program, IRCCS Azienda Ospedaliero-Universitaria di Bologna, Bologna, Italy; and [i]Centro Sindrome di Marfan e Aortopatie Ereditaria, Lancisi Cardiovascular Center, Azienda Ospedaliero-Universitaria delle Marche, Ancona, Italy.

Institutional Review Board: EM624-2019_246/2016/O/Oss/AOUBo.

Read at the IRCCS Azienda Ospedaliero-Universitaria di Bologna, Italy; Lancisi Cardiovascular Center, Ancona, Italy.

Received for publication Oct 16, 2023; revisions received March 17, 2024; accepted for publication March 19, 2024; available ahead of print May 15, 2024.

Address for reprints: Luigi Lovato, MD, Pediatric and Adult Cardiothoracic and Vascular, Oncohematologic and Emergency Radiology Unit, IRCCS Azienda Ospedaliero-Universitaria di Bologna, via Massarenti 9, 40138 Bologna, Italy (E-mail: luigi.lovato@aosp.bo.it).

2666-2736

https://doi.org/10.1016/j.xjon.2024.03.015

Abbreviations and Acronyms

AA = ascending aorta
AR = aortic root
AUC = area under the curve
BSA = body surface area
CTA = computed tomography angiography
HTAD = heritable thoracic aortic disease
IQR = interquartile range
LDS = Loeys-Dietz syndrome
MFS = Marfan syndrome
MRA = magnetic resonance angiography
ROC = receiver operating characteristic
STJ = sinotubular junction

The understanding of aortic disease has grown in the past decades. Among the young adult and adolescent population, hereditary aortic diseases represent a distinct yet clinically significant group of conditions.[1-3] Identification of specific genes associated with hereditary thoracic aortic aneurysm and dissection has defined molecular mechanisms underlying aneurysm formation, highlighting the scientific and clinical attention to these entities.[4,5] However, individuals with hereditary thoracic aortic diseases may remain undiagnosed, resulting in a substantial healthcare burden. Marfan syndrome (MFS) and Loeys-Dietz syndrome (LDS) stand as the 2 more frequent forms of hereditary thoracic aortic disease (HTAD). MFS typically arises from heterozygous mutations in FBN1, a gene responsible for encoding the extracellular matrix protein fibrillin-1. Its predominant cardiovascular manifestation involves aortic aneurysms and dissections in the sinuses of Valsalva. On the other hand, LDS is associated with mutations in TGBR1/2, SMAD2/3, or TGFB2/3, genes that encode components of the transforming growth factor-β signaling pathway. Both syndromes exhibit marked pleiotropism, displaying variable manifestations of skeletal, ocular, and cardiovascular defects, with the latter contributing most significantly to morbidity and mortality, impacting prognosis and life expectancy.[6] Despite some characterizing features, phenotypical and clinical overlap between LDS and MFS can occur in patients, as well as among young adults and especially athletes with tall stature, causing unrecognition or delay in diagnosis and treatment.[7] Compared with MFS, cardiovascular manifestations in LDS tend to be more severe and aggressive.[8] Thus, timely and accurate diagnosis is paramount to enhance a patient's survival prospects and prevent severe complications. For many years, echocardiography was the only imaging technique used to evaluate aortic involvement in HTAD. Recently, evolution of total body imaging techniques has led to a wider definition of vascular involvement in these disorders.[9] Nevertheless, a systematic comparison of the aortic anatomy of patients with LDS and MFS has never been considered. The aim of this study was to analyze segmental differences in aortic morphology between 2 cohorts of patients with LDS and MFS, with the goal of identifying distinctive features of aortic involvement and specific aortic anatomic profiles.

MATERIAL AND METHODS

Study Subjects and Design

A multicenter observational retrospective analysis of aortic morphology was conducted in patients with a confirmed diagnosis of LDS and MFS who underwent magnetic resonance angiography (MRA) or computed tomography angiography (CTA) of the aorta at the time of diagnosis or during initial clinical and imaging follow-up by 2 Nationwide Marfan and Heritable Rare Thoracic Aortic Diseases Hub centers (Bologna and Ancona, Italy) from July 2006 to August 2020. The study was approved by the local ethics committee (EM624-2019_246/2016/O/Oss/AOUBo, July 17, 2019). Informed consent was obtained from all study participants in accordance with the Declaration of Helsinki and national legal regulations. All patients with LDS had a confirmed pathogenic variant in 1 of the 6 genes known to be responsible for the disease (TGBR1/2, SMAD2/3, or TGFB2/3). The diagnostic criteria for patients with MFS were a confirmed pathogenic variant in FBN1 gene and a clinical diagnosis according to the revised Ghent nosology.[10,11] A total of 270 patients with MFS and 55 patients with LDS were screened for enrollment. Exclusion criteria were age less than 18 years (pediatric patients were excluded to account for completely grown-up aortic morphology), insufficient imaging quality due to motion artifacts and incomplete examinations (absence of a 3-dimensional volume setting of contrast-enhanced or unenhanced MRA), and a history of thoracic aortic surgical/endovascular treatment or aortic dissection at the time of enrollment without a previous CTA or MRA available. In addition, when the first CTA or MRA available was close to aortic surgical intervention or showed large aortic aneurysms, the patient was excluded as an expression of an advanced aortic disease, avoiding potential selection bias.

A total of 114 patients from the original dataset were enrolled, 95 with MFS and 19 with LDS. The aortic morphology was evaluated comparing aortic diameters, lengths, areas, tortuosity, anatomic variants, and arch type prevalence between the 2 groups. Additional measurement (length and diameters) ratios were considered. The thoracic aorta morphology was also analyzed comparing the 2 groups with a third cohort of 20 age- and sex-matched controls with no history and no evidence of aortic disease. Clinical and epidemiological data were obtained from the outpatient medical reports for all the patients visited in the Marfan centers, and the comparative analysis between the 2 cohorts is summarized in Table 1.

Imaging Analysis

MRA was performed with two 1.5-Tesla MR scanners (General Electric Medical System and Philips Medical Systems), and CTA was conducted by a 16,128 and 192 $\times$ 2-channel scanners (Siemens Healthineers and Philips Medical Systems). In our center, we perform MRA as the first choice to reduce the dose radiation burden in a relatively young population. CTA was used alternatively because of the higher system availability. A complete detailed description concerning imaging techniques and protocols, aortic segmentation, and measurements methodology is presented in the Appendix E1 section. MRA and CTA protocols always included a 3-dimensional angiographic arterial acquisition of the thoracoabdominal aorta from the proximal supra-aortic vessels to the femoral bifurcation level. The thoracoabdominal aorta was divided into several segments following widespread clinical practice. The ascending aorta (AA) was measured at 3 levels: proximal AA, pulmonary bifurcation level, and distal AA. The aortic diameter measurements were performed according to the most recent international guidelines[12,13] on at least 2 perpendicular planes

TABLE 1. Clinical and demographic features of Marfan syndrome and Loeys-Dietz syndrome cohorts

Baseline characteristics	LDS (n = 19)*	MFS (n = 95)*	*P*
Age at examination (y)	44 (32-52)	34 (25-46)	.070
Weight (kg)	63 (60-78)	70 (60-78)	.486
Height (m)	1.70 (1.63-1.76)	1.80 (1.73-1.90)	**<.001**†
BSA (m^2)	1.76 (1.68-1.85)	1.90 (1.74-2.07)	**.020**
Gender (female)	14 (73.7%)	51 (53.7%)	.100
Imaging modality (CTA)	13 (68.4%)	48 (50%)	.150
Imaging modality (MR)	12 (63.2%)	68 (71.6%)	.460
Obesity/overweight	4 (21.1%)	4 (4.2%)	**.020**
Smoking	0	8 (8.6%)	.250
Hypertension	1 (5.3%)	5 (5.4%)	.730
Diabetes	0	0	-
Hypercholesterolemia	2 (10.5%)	7 (7.5%)	.470
AoR	3 (18.8%)	32 (36%)	.250
Familial history of sudden death	7 (36.8%)	28 (29.8%)	.540
Familial history of aortic aneurysm	12 (66.7%)	16 (17%)	**<.001**
Familial history of AD	6 (31.6%)	19 (20.2%)	.276
Combined family history of aortic disease/sudden death	15 (78.9%)	43 (45.7%)	**.007**
Aortic dilation prevalence‡	10 (52.6%)	76 (80%)	**.0**11
Aortic arch type 2-3	31 (32.6%)	10 (52.6%)	.097

LDS, Loeys-Dietz syndrome; *MFS*, Marfan syndrome; *BSA*, body surface area; *CTA*, computed tomography angiography; *MR*, magnetic resonance; *AoR*, aortic regurgitation; *AD*, aortic dissection; *IQR*, interquartile range. *Values are expressed as median (IQR) or number (%). †Statistically significant values are marked by bold numbers. ‡AR and AA level.

using multiplanar reformatted reconstructions with manual delineation and confirmed by the semiautomated Arterial Vessel Analysis software (Intelli Portal, Philips) that provides double oblique transverse-oriented images for every point of the selected aortic segment. The aortic root (AR) diameters were calculated measuring the 3 sinus-to-sinus distances (intercoronary, left coronary–noncoronary, right coronary–noncoronary) at the point of maximum expansion to search for potential asymmetries. A per-segment analysis as well for total thoracoabdominal aorta was performed for length, tortuosity index, and area calculations. All these measurements were applied using the Arterial Vessel Analysis software. The centerline approach was used for length and tortuosity measurements. The arch type was defined following the interventional classification proposed by Marrocco-Trischitta and colleagues,[14] based on the ratio between the distance of the innominate artery ostium from the top of the aortic arch and the left common carotid artery caliber: A value less than 1 indicates type I, greater than 2 indicates type III, and between 1 and 2 indicates type II arch. The larger the distance from the top of the arch, the higher the degree of the aortic arch slope. The elongated transverse aortic arch was identified following Kim and colleagues' definition.[15] A retrospective review of all MRA or CTA examinations was independently conducted by 2 experienced readers (radiologists expert on cardiovascular imaging). Image quality was used to choose which imaging modality to perform the measurements in patients in whom both CTA and MRA were available. When this was equal, we preferred the computed tomography measures, because they are easier to handle.

Statistical Analysis

All analyses were conducted in SPSS version 23 (SPSS Inc), Microsoft Windows version. Normality of data distribution was examined with the Kolmogorov–Smirnov test. Continuous variables are expressed as mean ± SD or median with interquartile range as appropriate; the second system has been used systematically due to several variables without a normal distribution for all groups. Categorical variables are expressed as a percentage. For the continuous variables, comparisons between 2 groups were made using *t* tests, whereas for 3 or more groups with analysis of variance and Bonferroni test for multiple comparisons. The analysis of nonparametric variables used the Mann–Whitney test, whereas for 3 or more groups the Kruskal–Wallis test was used. For categorical variables, we used the chi-square test. The most significant continuous variables were first tested for linearity of the association with pathologies using restricted cubic splines receiver operating characteristic (ROC) analyses constructed to identify the most appropriate cut-off value to discriminate between the 2 populations.

RESULTS

A total of 95 patients with MFS and 19 patients with LDS were included in the final analysis. The 2 cohorts were similar in age, sex, and imaging modality used for the aorta examination. There were no statistically significant differences for all the comorbidities potentially affecting aortic morphology except a larger proportion of obesity among LDS (21% vs 4% $P = .02$) and a greater body surface area (BSA) in MFS (median and interquartile range [IQR], 1.9 m^2, 1.74-2.07 m^2 vs 1.76, 1.68-1.85 m^2; $P = .02$) as foreseen. Patients with MFS showed a higher

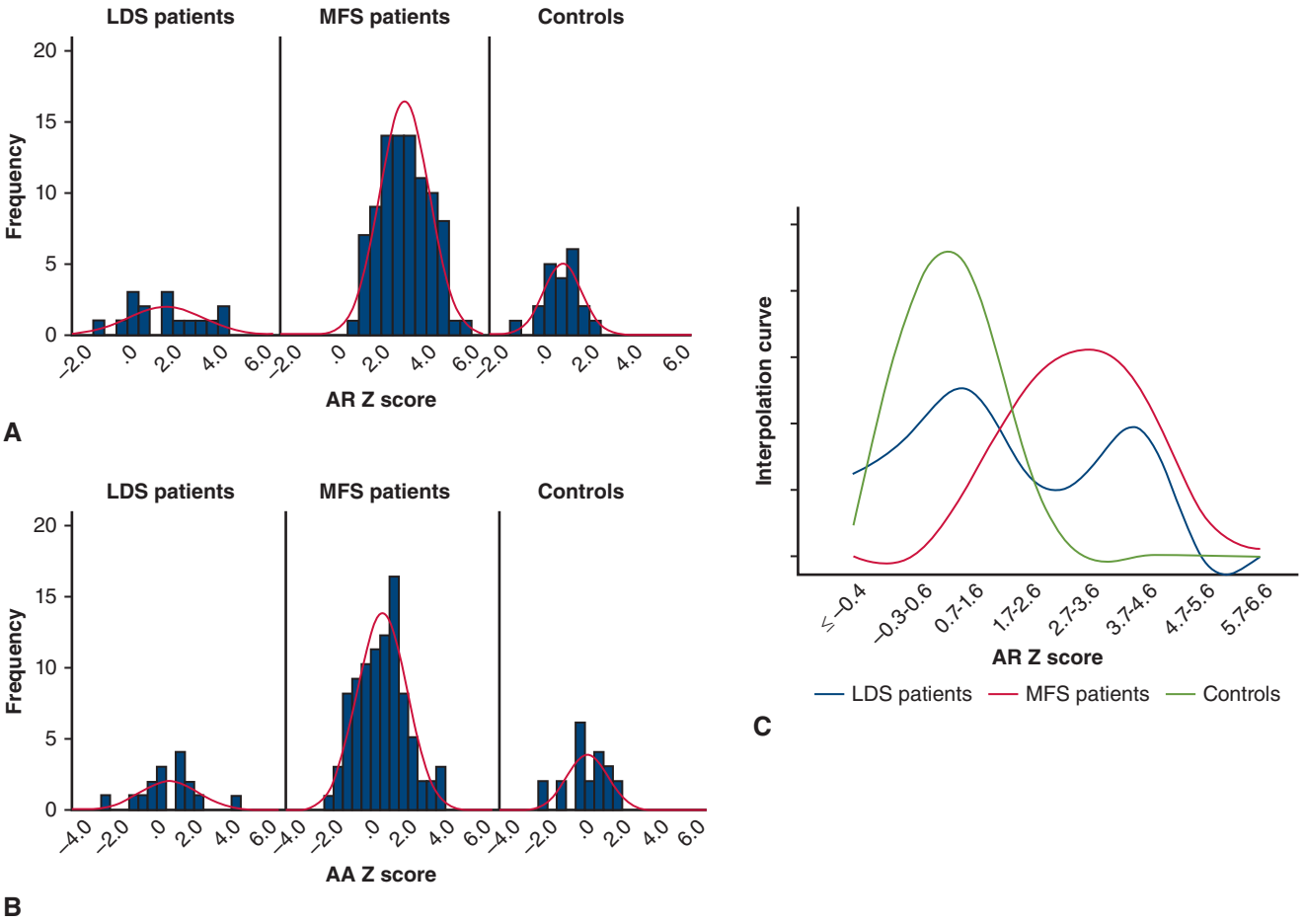

FIGURE 1. AR, AA Z-score frequency distribution in MFS, LDS, and controls. A, Value +2 or greater indicates aortic dilation. Net distribution of MFS AR diameters to the right of +2 value indicates strong prevalence of dilated aorta. Controls show an opposite distribution. LDS values are equally distributed on both sides of the +2 value. B, Same representation for AA diameters shows more similar value distribution between LDS and MFS. C, AR Z-score value distribution represented by interpolation splines shows a net separation between MFS and controls. LDS 2-*peak shape curve* indicates a larger overlapping with normal subjects. *LDS*, Loeys-Dietz syndrome; *MFS*, Marfan syndrome; *AA*, ascending aorta; *AR*, aortic root.

prevalence of AA and AR dilation (82% vs 50%, $P = .011$), intended as Z-score +2 or greater, calculated by following Campens' normograms.[16] Conversely, among clinical and epidemiological features, the LDS group differed significantly for its stronger familial history of aortic aneurysms (prevalence 66.7% vs 17%, $P < .001$) and the combined aortic pathology and sudden death events. All baseline features are summarized in Table 1.

Comparative Analysis of Aortic Dilation

The MFS group showed diffusely larger aortic dimensions compared with the LDS cohort, especially at the AR and suprarenal level, but also AA and isthmus, with significantly greater values of all the 3 sinus-to-sinus diameters (median and IQR: 40 mm, 36-43.25 vs 36.5 mm, 30.2-40.5 mm for left-to-right coronary sinus diameter, $P = .005$) and both coronal and sagittal measures of suprarenal abdominal aorta (median and IQR: 19 mm, 14-20 mm vs 15 mm, 13-17.75 and 19.5 mm, 16-22 mm vs 17 mm, 14.25-19 mm, respectively; $P < .05$), confirmed after adjusting the aortic diameters for BSA (median and IQR noncoronary to right sinus diameter 21.06 mm/m^2, 19.48-22.8 mm/m^2 vs 18.52 mm/m^2, 16.4-22.77 mm/m^2, $P = .041$). Patients with MFS also have greater iliac artery dimensions and a higher prevalence of iliac artery dilatation (18.1% vs 10.5%), especially the left iliac artery (14.9% vs 5.3%), whereas the LDS group had larger values in the distal arch and middle-to-distal descending thoracic aorta. The distribution of Z score values for AR and AA among the 3 cohorts are illustrated by frequency histograms (Figure 1). The absolute and BSA-indexed aortic diameters distribution and relative differences are also represented by box plots for AR, sinotubular junction (STJ), and AA in the same cohorts (Figure 2). A clear distinction of MFS values from both LDS and controls is evident for AR diameters. The LDS group shows larger overlapping of aortic

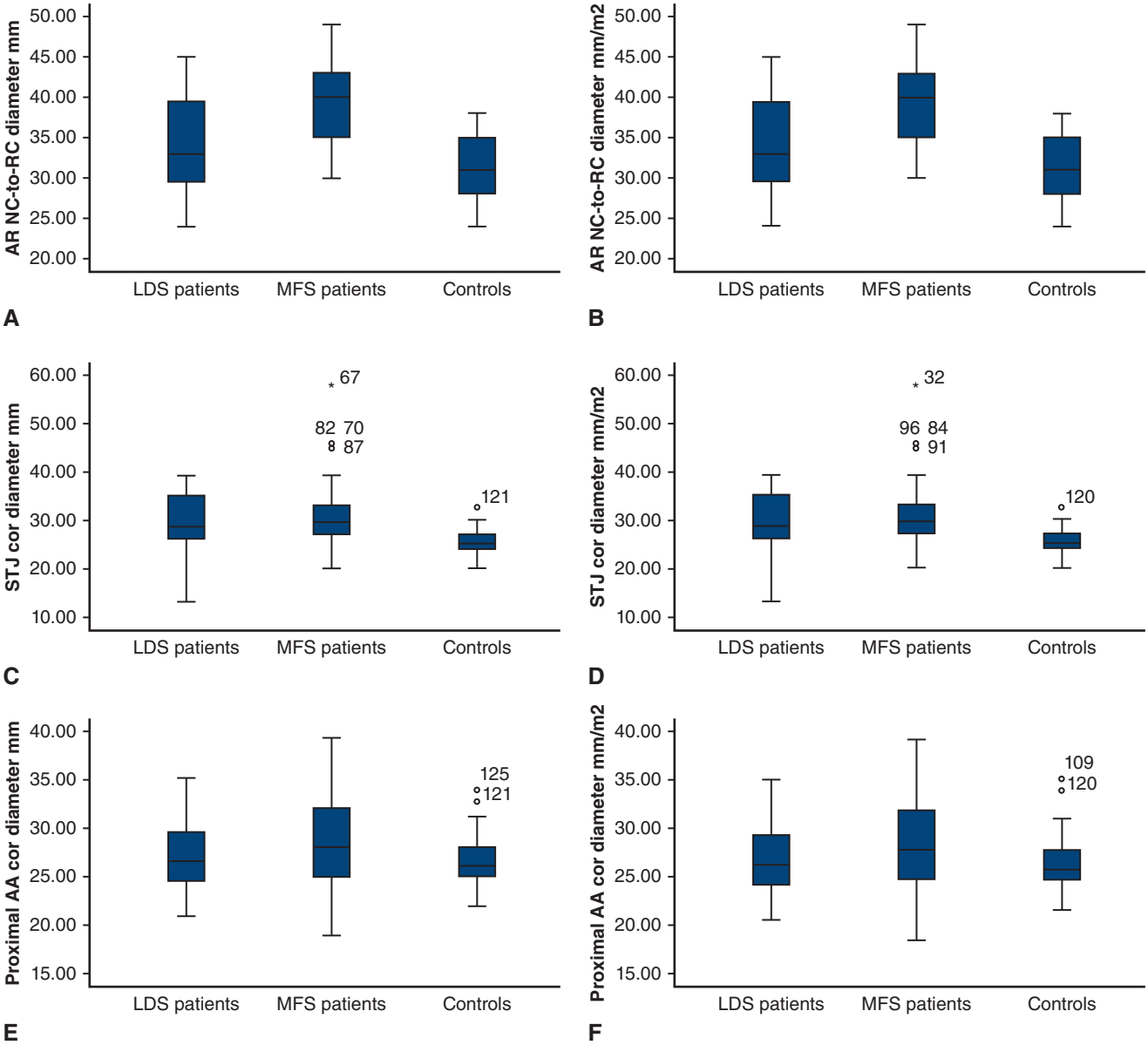

FIGURE 2. Proximal aortic segments dimensional profile in LDS, MFS, and controls. Absolute and size-indexed diameter box-plot representations for NC-to-RC (A and B), coronal STJ (C and D), and coronal AA (E and F). MFS AR diameters are distinct from the other groups; larger overlapping is evident between LDS and controls (A and B). Both syndromes show higher STJ diameters than controls, overlapping completely each other (C and D). LDS and MFS AA diameters are similar, but LDS more largely overlaps with controls showing almost the same median value (E and F). Lower and upper box borders represent 25th and 75th percentiles. The *middle horizontal lines* represent the median. The lower and upper whiskers represent minimum and maximum values of nonoutliers. Extra *dots* (*,°) mark the outliers. *AR*, Aortic root; *NC*, noncoronary sinus; *RC*, right coronary sinus; *LDS*, Loeys-Dietz Syndrome; *MFS*, Marfan syndrome; *STJ*, sinotubular junction; *cor*, coronal; *AA*, ascending aorta.

dimensions with controls, with similar median values in AA. The comparison of the whole spectrum of absolute and BSA-indexed thoracoabdominal aorta diameters is shown in Table E1. Box-plot representations of aortic absolute diameters comparison of the whole thoracoabdominal aorta among our cohorts are displayed by Figure E1.

Morphologic Parameters

The MFS group has a significantly longer AR measured from the aortic annulus to the STJ (median and IQR: 26 mm, 23-29 mm vs 22 mm, 20-26 mm; $P = .013$). AR asymmetries are equally distributed in both syndromes, representing 25% to 30% of cases. Patients with LDS show

TABLE 2. Aortic segments lengths and main morphologic patterns in Marfan syndrome and Loeys-Dietz syndrome cohorts

	Aortic lengths (mm)*			Aortic indexed lengths (mm/m^2)*		
Aortic segments	**LDS patients (n = 19)**	**MFS patients (n = 95)**	***P***	**LDS patients (n = 19)**	**MFS patients (n = 95)**	***P***
AR	22 (20-26)	26 (23-29)	.013	14.1 (12.9-14.5)	13.5 (11.8-15.8)	.973
AA	65 (56-79)	65 (56-73)	.843	35 (32-42)	35 (29-39)	.133
Aortic arch	37 (30-46)	32 (25-39)	.053	21 (17-26)	16 (13-20)	.006
Aortic isthmus	28 (20-34)	31 (25-38)	.063	15 (11-20)	16 (14-20)	.382
DTA	142 (131-167)	153 (142-166)	.110	83.5 (77-98)	80 (75-87)	.110
Suprarenal aorta	80 (61-96)	69 (56-80)	.038	45 (35-57)	37 (30-41)	.003
Infrarenal aorta	91 (79-107)	98 (84-116)	.143	51 (48-56)	53 (44-60)	.646
Right iliac artery	67 (57-84)	63 (55-98)	.361	36 (27-47)	35 (29-43)	.933
Left iliac artery	66 (52-83)	62 (54-97)	.884	39 (33-49)	36 (28-44)	.240

Aortic arch morphology	**LDS patients (n = 19) N (%)**	**MFS patients (n = 95) N (%)**	***P***
Aortic arch anomalies	0	2 (2.1%)	.690
Arch elongation	4 (21.1%)	10 (10.5%)	.182
Type 2-3 aortic arch	10 (52.6%)	31 (32.6%)	.097

LDS, Loeys-Dietz syndrome; *MFS*, Marfan syndrome; *AR*, aortic root; *AA*, ascending aorta; *DTA*, descending thoracic aorta; *IQR*, interquartile range. *Values are expressed as median (IQR).

longer length in several aortic segments, in particular longer aortic arch and suprarenal aorta (median and IQR: 37 mm, 30-46 mm vs 32 mm, 25-39 mm; $P = .053$ and 80 mm, IQR 61-96 mm vs 69 mm, 56-80 mm, $P = .038$). Type 1 aortic arch is prevalent in the MFS group (67.4% vs 47.4%), and patients with LDS show a larger representation of type 2 to 3 aortic arch (52.6% vs 32.6%) and elongated aortic arch. The length measurements and aortic arch morphologic patterns are summarized in Table 2. No significant differences were noted in tortuosity index. The complete dataset concerning areas and tortuosity index are presented in Table E2. Among the additional measurement ratios considered in the comparative analysis of aortic morphology, the AR-to-AA length/AR diameter ratio is significantly lower in the MFS population than in the LDS population, whereas the AR/STJ and AR/AA diameter ratios are significantly higher in the MFS population. These simple morphometric ratios could help to differentiate the 2 syndromes. The same analysis has been repeated between the 2 cohorts according to the presence/absence of AR or AA dilation. The significant differences of these measurement ratios between the MFS and LDS populations have been confirmed among the patients without associated aortic dilation (median and IQR: AR-to-AA length/AR diameter 2.12, 1.94-2.28 vs 2.3, 2.15-2.63, $P = .043$, AR/STJ diameter 1.24, 1.18-1.34 vs 1.10, 1.06-1.37; $P = .05$ and AR/AA diameter, 1.26, 1.07-1.33 vs 1.06, 1.0-1.18; $P = .03$, respectively). This result is of great relevance, reinforcing the idea of the discriminating role of these morphologic indices especially at early aortic disease stages, suggesting their preemptive value considering the higher risk profile for aortic events in LDS. A further confirmation of the diagnostic value of these morphologic ratios comes from their interpolation curves that identify cutoff values able to differentiate the 2 syndromes, especially cut-off values have been identified for AR/STJ ($\geq$1.19) and AR/AA diameter ratios ($\geq$1.15) Specificity, positive predictive value, and negative predictive value are 63%, 91.3% and 35.3% and 58%, 90.4%, 35.5%, respectively.

The corresponding ROC curves illustrate a sensitivity to differentiate LDS from MFS of 76% (area under the curve [AUC], 0.69; 95% CI, 0.54-0.83) and 79% (AUC, 0.724; 95% CI, 0.58-0.86), respectively (Figure 3). Moreover, the aortic isthmus/descending thoracic aorta diameter ratio was greater in MFS than in LDS among patients with aortic dilation (median and IQR: 1.21, 1.11-1.27 vs 1.08, 1.03-1.09; $P = .015$). The most relevant morphometric indices are summarized in Table 3. Spline interpolation and ROC curves of AR-to-AA length/AR diameter ratio are shown in Figure E2.

DISCUSSION

MFS and LDS are the most common and clinically relevant HTADs. Both syndromes result from extracellular matrix component alterations and share a marked genetic heterogeneity and pleiotropism. More than 1800 mutations of the FBN1 gene have been recognized in MFS,[17,18] and LDS is characterized by mutation of several genes all coding for transforming growth factor-β signaling components.[19,20] Cardiovascular manifestations and especially aortic complications account for the highest mortality and morbidity rates in both syndromes.[21,22] Notably, LDS tends

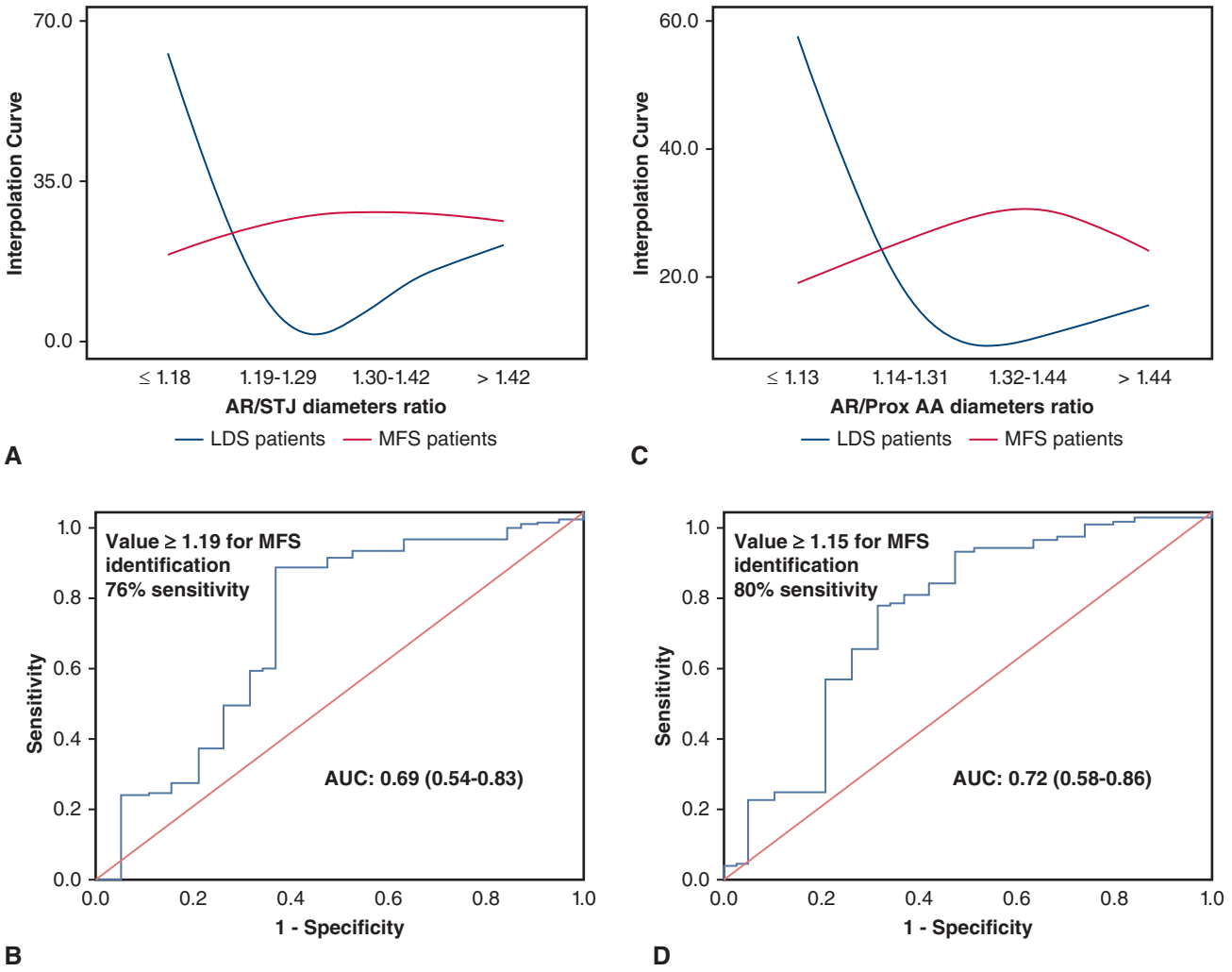

FIGURE 3. Performance of the main morphologic indices for LDS and MFS differential diagnosis. Spline interpolation and corresponding ROC curves of AR/STJ diameters ratio (A and B) and AR/Prox AA diameters ratio (C and D) in LDS and MFS populations. Spline interpolation illustrates the discrimination effect of the cutoff value, and the ROC curves quantify their accuracy. *LDS*, Loeys-Dietz syndrome; *MFS*, Marfan syndrome; *AR*, aortic root; *STJ*, sinotubular junction; *AUC*, area under the curve; *AA*, ascending aorta.

to manifest with greater severity, often leading to aortic dissection at an earlier age and at smaller aortic diameters, as evidenced by a lower median survival.[22-24] Life expectancy has been progressively improved in MFS by early diagnosis and prophylactic surgical AR replacement based on aortic diameter measurements.[25] Therefore, early recognition could have beneficial effects in terms of survival and disease management. Despite some distinctive and at times striking features, such as elongated arm span or arachnodactyly in MFS and the unique presence of hypertelorism, bifid uvula, or cleft palate in LDS, both syndromes exhibit considerable phenotypic overlap. This has been affirmed by the recent recognition of LDS as a distinct entity.[19,26] Moreover, specific characteristics such as widespread arterial aneurysms and peripheral vascular tortuosity in LDS[27,28] or musculoskeletal characteristics in MFS often account for no more than 30% to 50% of subjects.[29] The marked variability of disease phenotypic expression may hamper their distinction from normal subjects, especially in the context of tall stature athletes.

Morphologic Indexes in the Differential Diagnosis

Our study confirms the preeminent dilation of the AR and AA in both syndromes with a significantly higher prevalence of aortic dilation in MFS. Additionally, the predominant arch morphologies in LDS were types 2 and 3, which are closer to the "gothic" arch geometry and have a higher risk of type B dissection.[14,30,31] The elongated aortic arch is also more prevalent in patients with LDS, and it is another feature potentially associated with a more severe aortic disease. These aspects correspond to the literature evidence of a more severe course of cardiovascular alterations in

TABLE 3. Thoracic aorta measurements ratios (all patients, dilated aorta, not dilated aorta)

Morphologic ratios	All patients			Dilated aorta*			Not dilated aorta		
	LDS patients† (n = 19)	MFS patients† (n = 95)	*P*	LDS patients† (n = 8)	MFS patients† (n = 75)	*P*	LDS patients† (n = 11)	MFS patients† (n = 20)	*P*
AR-AA length/AR diameter	2.21 (1.87-2.51)	1.96 (1.72-2.21)	.002	1.86 (1.74-2.25)	1.94 (1.71-2.21)	.799	2.3 (2.15-2.63)	2.12 (1.94-2.28)	.043
AA length/AA diameter	2.20 (2.00-2.39)	2.18 (1.94-2.50)	.997	2.16 (2.06-2.37)	2.16 (1.96-2.5)	.938	2.20 (2.00-2.39)	2.10 (1.85-2.52)	.918
AR diameter/STJ diameter	1.13 (1.07-1.13)	1.30 (1.20-1.42)	.009	1.18 (1.07-1.40)	1.32 (1.20-1.45)	.112	1.13 (1.06-1.37)	1.24 (1.18-1.34)	.052
AR diameter/AA diameter	1.06 (1.025-1.31)	1.33 (1.20-1.43)	.002	1.27 (1.03-1.44)	1.34 (1.21-1.46)	.273	1.06 (1.00-1.18)	1.27 (1.07-1.33)	.030
AA diameter/DTA diameter	1.52 (1.39-1.66)	1.47 (1.35-1.61)	.152	1.63 (1.42-1.99)	1.50 (1.36-1.70)	.130	1.50 (1.39-1.60)	1.27 (1.07-1.33)	.011
Isthmus diameter/ DTA diameter	1.11 (1.07-1.20)	1.16 (1.06-1.25)	.344	1.08 (1.03-1.09)	1.21 (1.11-1.27)	.015	1.13 (1.07-1.20)	1.10 (1.02-1.18)	.090

LDS, Loeys-Dietz syndrome; *MFS*, Marfan syndrome; *AR*, aortic root; *AA*, ascending aorta; *STJ*, sinotubular junction; *DTA*, descending thoracic aorta; *IQR*, interquartile range.
*Dilated aorta refers to patients with AA or AR dilation. †Values are expressed as median (IQR).

LDS.[24,32] The per-segment analysis of aortic dimensions in LDS revealed a larger distribution of normal values. We observed a clear distinction between patients with MFS and normal subjects, whereas LDS values may overlap with the normal pattern (Figures 1 and 2; Table E1), revealing itself as a more insidious syndrome. Therefore, aortic tortuosity or arch elongation observed in LDS despite normal diameters as comprehensive aortic phenotypic tools may represent a first red flag of disease suspicion in the normal population, which in our control series lacks these morphologic features. The analysis of measurement ratios, especially at the level of AR and AA complex, was performed to highlight the morphologic differences evidenced between LDS and MFS. AR-to-AA length/AR diameter was significantly lower in MFS, whereas AR/STJ and AR/AA diameters were larger in patients with MFS. The corresponding ROC curves illustrate the discrimination power of the cutoff values identified for these indices with a sensitivity up to 80% for the AR/AA diameter ratio and AUC 0.724 with 95% CI 0.58-0.86 (Figures 3 and 4).

Clinicopathological Impact of Aortic Phenotypes

Our analysis revealed the exceptional discriminatory power of these ratios (Figure 4), especially in patients lacking aortic dilation at these levels. This emphasizes the presence of a distinct aortic phenotype before dilation occurs, signifying an early stage of aortic involvement in these diseases. Traditional clinical and imaging criteria often struggle to differentiate at this phase when genetic test results might not be readily available or conclusive. Early recognition of these syndromes could significantly enhance medical therapies, potentially maximizing their protective effect when initiated before advanced aortic disease sets in.[33] These morphologic ratios are rapidly calculated using different imaging modalities and could be easily applied during the normal clinical practice both at tertiary or hub imaging centers and peripheral or secondary medical sites. Our analysis also sheds light on the comprehensive morphology of the aorta and its primary segments, transcending mere aortic diameters. Particularly noteworthy is the proximal aorta complex; in MFS, it not only widens but also significantly elongates, assuming a distinctive "pear-shaped" configuration on dilation (Figure 4). This unique morphotype, especially in the sinuses of Valsalva, could serve as a visual clue, raising strong suspicions of the underlying disease. Conversely, LDS lacks significant AR morphology alterations, maintaining normal anatomic relationships even when dilated. The MFS cohort showed larger aortic diameters at several other segments, such as the isthmus, suprarenal aorta, and iliac arteries. The isthmus dilation is typical when the AA is already dilated and could represent another syndrome-specific phenotype. This morphotype could be a potential indicator of a more advanced disease status. Conversely, patients with LDS displayed longer aortic segments, especially in the aortic arch and abdominal aorta, reflecting aortic tortuosity, a hallmark of LDS. The main imaging morphologic indices and aortic phenotypes useful for LDS and MFS distinction are summarized in Table 3. These distinct aortic morphotypes, observed at various stages of hereditary thoracic aortic diseases, serve as practical tools for differentiation. They potentially reflect the diverse impact of pathogenetic mechanisms involving fibrillin 1 and transforming growth factor-β on different aortic sections and their developmental processes, contributing to a deeper understanding of these intricate diseases.[34]

In the realm of thoracic aortic aneurysm and dissection, where 37 genes are associated with genetic variants or

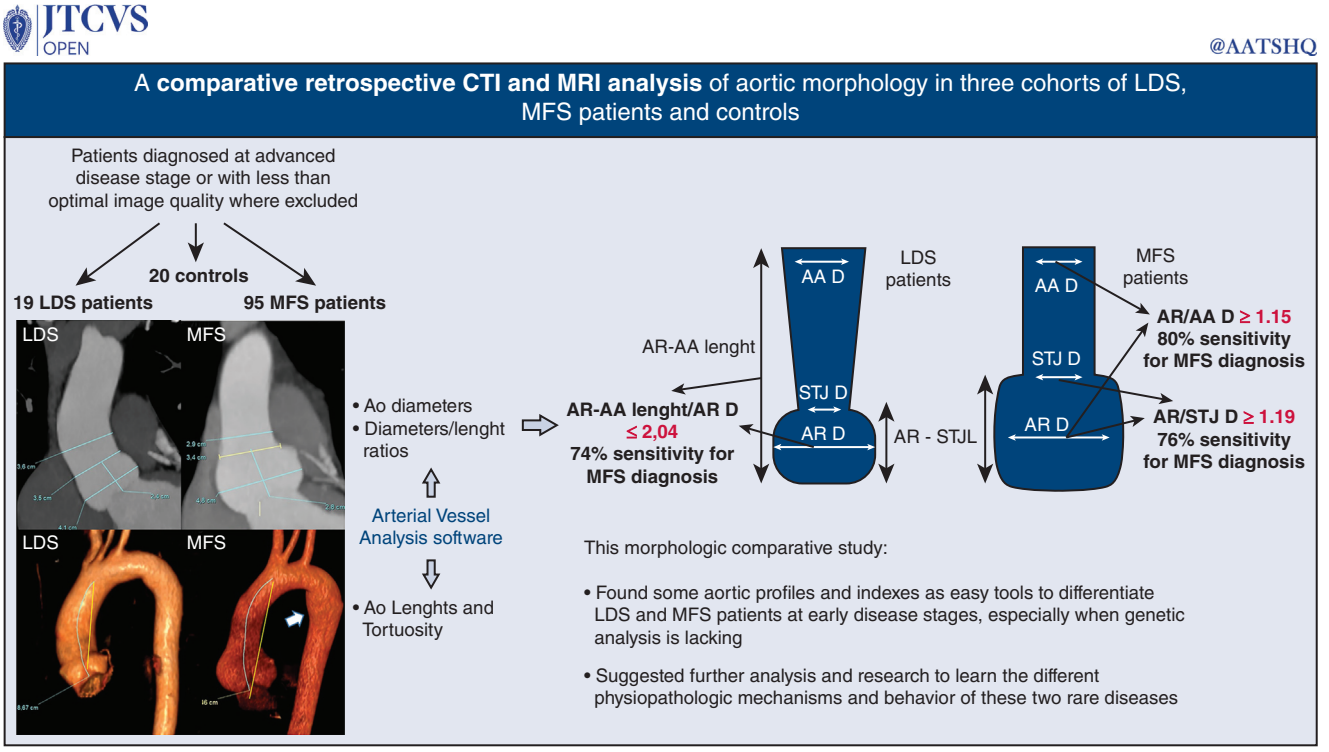

FIGURE 4. Computed tomography and magnetic resonance imaging aortic morphology analysis provides aortic profiles and indices as early tools to differentiate patients with LDS and MFS. Aortic diameter, length, and tortuosity measurements are performed in selected cohorts of LDS, MFS, and controls; the main derived diameter or diameter/length ratios for AR and AA in patients with LDS and MFS are shown on representatives computed tomography images on the *left*; the relative morphotypes, derived indices with cut-off values, and corresponding diagnostic accuracy are schematically represented on the *top right*. The main result and take-home messages are shown on the *bottom right*. *CTI*, Computed tomography imaging; *MRI*, magnetic resonance imaging; *LDS*, Loeys-Dietz syndrome; *MFS*, Marfan syndrome; *AR*, aortic root; *AA*, ascending aorta; *D*, diameter; *STJ*, sinotubular junction; *L*, length.

mutations,[35] many families with multiple affected members remain genetically elusive. For these patients, CTA and MRA aortic phenotyping could emerge as valuable tools, guiding surveillance and treatment decisions amid the complexity of genetic variability.

Study Limitations

The retrospective nature of the study has limited partly the number of patients analyzed. Some advanced statistical analysis could not be conducted for the limited number of cohorts. A possible selection bias may result from the exclusion of many patients who came to our centers when already surgically treated and whose previous CTA or MRA results were not available. These patients could represent a higher-risk population with specific anatomic patterns. Morphologic differences also may reflect the diverse impact of some specific genotypes, but a genotype/phenotype correlation analysis was beyond the aim of our study. Finally, the potential impact in the prognosis of these anatomic differences is crucial but needs a focused long-term follow-up.

CONCLUSIONS

Both syndromes show peculiar anatomical patterns at different aortic levels irrespective of aortic dilation and disease severity. These aortic profiles and indexes could be used as easy tools to help differentiate MFS and LDS patients at early disease stages and may represent the expression of different genetic mutations on aortic development, with potential impact on prognosis and possibly contributing to better management of the diseases The systematic adoption of whole body imaging with MRI or CT should always be considered, as they allow a complete vascular assessment with practical indicators of differential diagnosis.

Conflict of Interest Statement

The authors reported no conflicts of interest.

The *Journal* policy requires editors and reviewers to disclose conflicts of interest and to decline handling or reviewing manuscripts for which they may have a conflict of interest. The editors and reviewers of this article have no conflicts of interest.

Dr Lovato thanks Dr Chiara Nocera for producing and providing the drawing of global aorta morphotypes.

References

1. Cury M, Zeidan F, Lobato AC. Aortic disease in the young: genetic aneurysm syndromes, connective tissue disorders, and familial aortic aneurysms and dissections. *Int J Vasc Med*. 2013;2013:267215.

2. Karakurt C. Aortic aneurysm in children and adolescents. In: Aortic Aneurysm - Recent Advances [Internet]. IntechOpen; 2013. Accessed September 28, 2023. https://www.intechopen.com/chapters/44134
3. Papatheodorou E, Degiannis D, Anastasakis A. Genetics of heritable thoracic aortic disease. *Cardiogenetics*. 2022;12(1):63-79.
4. Bararu Bojan Bararu I, Pleșoianu CE, Badulescu OV, et al. Molecular and cellular mechanisms involved in aortic wall aneurysm development. *Diagnostics*. 2023; 13(2):253.
5. Bhandari R, Aatre RD, Kanthi Y. Diagnostic approach and management of genetic aortopathies. *Vasc Med*. 2020;25(1):63-77.
6. Cook JR, Carta L, Galatioto J, et al. Cardiovascular manifestations in Marfan syndrome and related diseases; multiple genes causing similar phenotypes. *Clin Genet*. 2015;87(1):11-20.
7. Willis L, Roosevelt GE, Yetman AT. Comparison of clinical characteristics and frequency of adverse outcomes in patients with Marfan syndrome diagnosed in adulthood versus childhood. *Pediatr Cardiol*. 2009;30(3):289-292.
8. Stengl R, Bors A, Ágg B, et al. Optimising the mutation screening strategy in Marfan syndrome and identifying genotypes with more severe aortic involvement. *Orphanet J Rare Dis*. 2020;15(1):290.
9. Roman MJ, Devereux RB. Diagnostic imaging of the cardiovascular system in the Marfan syndrome. *Prog Pediatr Cardiol*. 1996;5(3):175-188.
10. Suliman A, Yan W, Yamashita MH, et al. A previously undescribed pathogenic variant in FBN1 gene causing Marfan syndrome: a case report. *Eur Heart J Case Rep*. 2022;6(3):ytac063.
11. Pereira JP, Ferreira JR, Botelho APA, et al. Identification of a novel pathogenic variant in FBN1 associated with Marfan Syndrome. *Cold Spring Harb Mol Case Stud*. 2022;8(4):a006215.
12. Erbel R, Aboyans V, Boileau C, et al. 2014 ESC Guidelines on the diagnosis and treatment of aortic diseases: document covering acute and chronic aortic diseases of the thoracic and abdominal aorta of the adult. The Task Force for the Diagnosis and Treatment of Aortic Diseases of the European Society of Cardiology (ESC). *Eur Heart J*. 2014;35(41):2873-2926.
13. Evangelista A, Sitges M, Jondeau G, et al. Multimodality imaging in thoracic aortic diseases: a clinical consensus statement from the European Association of Cardiovascular Imaging and the European Society of Cardiology working group on aorta and peripheral vascular diseases. *Eur Heart J Cardiovasc Imaging*. 2023;24(5):e65-e85.
14. Marrocco-Trischitta MM, Rylski B, Schofer F, et al. Prevalence of type III arch configuration in patients with type B aortic dissection. *Eur J Cardiothorac Surg*. 2019;56(6):1075-1080.
15. Kim HK, Gottliebson W, Hor K, et al. Cardiovascular anomalies in Turner syndrome: spectrum, prevalence, and cardiac MRI findings in a pediatric and young adult population. *AJR Am J Roentgenol*. 2011;196(2):454-460.
16. Campens L, Demulier L, De Groote K, et al. Reference values for echocardiographic assessment of the diameter of the aortic root and ascending aorta spanning all age categories. *Am J Cardiol*. 2014;114(6):914-920.
17. Sakai LY, Keene DR, Renard M, et al. FBN1: the disease-causing gene for Marfan syndrome and other genetic disorders. *Gene*. 2016;591(1):279-291.
18. Kayhan G, Ergun MA, Ergun SG, et al. Identification of three novel FBN1 mutations and their phenotypic relationship of Marfan syndrome. *Genet Test Mol Biomarkers*. 2018;22(8):474-480.
19. Gouda P, Kay R, Habib M, et al. Clinical features and complications of Loeys-Dietz syndrome: a systematic review. *Int J Cardiol*. 2022;362:158-167.
20. Bowdin SC, Laberge AM, Verstraeten A, et al. Genetic testing in thoracic aortic disease–when, why, and how? *Can J Cardiol*. 2016;32(1):131-134.
21. Jones JA, Ikonomidis JS. The pathogenesis of aortopathy in Marfan syndrome and related diseases. *Curr Cardiol Rep*. 2010;12(2):99-107.
22. Loeys BL, Dietz HC. Loeys-Dietz syndrome. In: Adam MP, Mirzaa GM, Pagon RA, et al., eds. *GeneReviews® [Internet]*. University of Washington; 1993. Accessed September 28, 2023. http://www.ncbi.nlm.nih.gov/books/NBK1133/
23. Teixidó-Tura G, Franken R, Galuppo V, et al. Heterogeneity of aortic disease severity in patients with Loeys-Dietz syndrome. *Heart*. 2016;102(8):626-632.
24. Martin CA, Clowes VE, Cooper JP. Loeys-Dietz syndrome: life threatening aortic dissection diagnosed on routine family screening. *BMJ Case Rep*. 2014; 2014:bcr2013203063.
25. Choudhary SK, Goyal A. Aortic root surgery in Marfan syndrome. *Indian J Thorac Cardiovasc Surg*. 2019;35(Suppl 2):79-86.
26. Loeys BL, Chen J, Neptune ER, et al. A syndrome of altered cardiovascular, craniofacial, neurocognitive and skeletal development caused by mutations in TGFBR1 or TGFBR2. *Nat Genet*. 2005;37(3):275-281.
27. Meester JAN, Verstraeten A, Schepers D, et al. Differences in manifestations of Marfan syndrome, Ehlers-Danlos syndrome, and Loeys-Dietz syndrome. *Ann Cardiothorac Surg*. 2017;6(6):582-594.
28. Nistri S, De Cario R, Sticchi E, et al. Differential diagnosis between Marfan syndrome and Loeys–Dietz syndrome type 4: a novel chromosomal deletion covering TGFB2. *Genes (Basel)*. 2021;12(10):1462.
29. Lipscomb KJ, Clayton-Smith J, Harris R. Evolving phenotype of Marfan's syndrome. *Arch Dis Child*. 1997;76(1):41-46.
30. Marrocco-Trischitta MM, Romarowski RM, de Beaufort HW, et al. The modified arch landing areas nomenclature identifies hostile zones for endograft deployment: a confirmatory biomechanical study in patients treated by thoracic endovascular aortic repair. *Eur J Cardiothorac Surg*. 2019;55(5):990-997.
31. Schoenhoff FS, Alejo DE, Black JH, et al. Management of the aortic arch in patients with Loeys-Dietz syndrome. *J Thorac Cardiovasc Surg*. 2020;160(5):1166-1175.
32. Mariucci E, Spinardi L, Stagni S, et al. Aortic arch geometry predicts outcome in patients with Loeys-Dietz syndrome independent of the causative gene. *Am J Med Genet A*. 2020;182(7):1673-1680.
33. Ammash NM, Sundt TM, Connolly HM. Marfan syndrome-diagnosis and management. *Curr Probl Cardiol*. 2008;33(1):7-39.
34. Sherif HMF. Heterogeneity in the segmental development of the aortic tree: impact on management of genetically triggered aortic aneurysms. *Aorta (Stamford)*. 2014;2(5):186-195.
35. Faggion Vinholo T, Brownstein AJ, Ziganshin BA, et al. Genes associated with thoracic aortic aneurysm and dissection: 2019 update and clinical implications. *Aorta (Stamford)*. 2019;7(4):99-107.

Key Words: aortic anatomy, aortic root, computed tomography, Loeys-Dietz syndrome, magnetic resonance angiography, Marfan syndrome

SUPPLEMENTARY METHODS

Imaging Analysis

MRA was performed on a 1.5 Tesla MR scanner (Signa, General Electric Medical System, from 2006 to 2015; Ingenia, Philips Medical Systems, from 2016 in Sant'Orsola; Signa, General Electric Medical System in Lancisi Cardiovascular Center). CTA was conducted on a multidetector computed tomography scanner (Sensation 16-rows Cardiac CT, Siemens Healthcare, from 2006 to 2012; 128-rows Brilliance ICT from 2013, Philips Medical Systems; Somatom Force 192 × 2 Dual Source CT in Lancisi Cardiovascular Center). The MR protocol included stacks of axial and sagittal oblique T1-weighted fast spin-echo images covering the whole thoracic aorta. Coronal balanced fast field echo (BFFE) stack for AR imaging and a complete thoracoabdominal aorta 3-dimensional dataset of contrast-enhanced MRA or alternatively unenhanced Navigator-echo 3-dimensional BFFE Dixon MRA. CTA of thoracoabdominal aorta was mainly acquired with a slice thickness of 0.5 mm. A retrospective review of all MRA or CTA examinations was independently conducted by 2 experienced readers (radiologists expert on cardiovascular imaging) with 2 and 20 years of experience, respectively. Image quality was used to choose which imaging modality to perform the measurements in patients in whom both CTA and MRA were available. When this was equal, we preferred the computed tomography measures, because they are easier to handle.

The thoracoabdominal aorta was divided into several segments following widespread used clinical practice. The AA was measured at 3 levels: proximal AA, 1 cm distal to STJ, and pulmonary bifurcation level and distal AA, 1 cm to innominate artery (IA). The aortic diameter measurements were performed according to the most recent international guidelines[E1,E2] on at least 2 perpendicular planes (oblique sagittal and coronal or transverse oriented) using multiplanar reformatted reconstructions with manual delineation and confirmed by the semiautomated Arterial Vessel Analysis (AVA) software (IntelliSpace Portal, Philips) that provides double oblique short-axis oriented images for every point of the selected aortic segment. Aortic diameters were measured at end-diastole, inner-to-inner edge at the level of AR and AA, whereas outer-to-outer edge was used when wall atheromasia or thrombus was present or in the distal aortic segments. The AR diameters were calculated measuring the 3 sinus-to-sinus distances (intercoronary, left coronary–noncoronary, right coronary–noncoronary) at the point of maximum expansion to search for potential asymmetries. Black-blood or BFFE imaging was evaluated when using magnetic resonance imaging to identify the aortic wall thickening and to measure aortic diameters, avoiding underestimation with the MRA technique. Length measurements included the total thoracic and abdominal aorta, and each identified segment. In particular, the AR extends from aortic annulus to STJ, the AA extends from STJ to IA, the aortic arch extends from IA to the left subclavian artery ostium, the isthmic aorta extends from left subclavian artery origin to the pulmonary bifurcation level, and the distal thoracic aorta until the diaphragmatic hiatus. The lengths, including upper-renal, subrenal aorta, and both common iliac arteries, were applied using the centerline approach through the AVA software. Each aortic segment area was also calculated using the AVA software. The aortic tortuosity semiquantification was performed calculating the ratio between the intraluminal (centerline) distance and the straight lines connecting the origin and the end of each segment or their summed distances if a group of segments or the total thoracic and abdominal aorta were considered.

E-References

E1. Erbel R, Aboyans V, Boileau C, et al. ESC Guidelines on the diagnosis and treatment of aortic diseases. *Eur Heart J*. 2014;35:2873-2926.

E2. Evangelista A, Sitges M, Jondeau G, et al. Multimodality imaging in thoracic aortic diseases: a clinical consensus statement from the European Association of Cardiovascular Imaging and the European Society of Cardiology working group on aorta and peripheral vascular diseases. *Eur Heart J Cardiovasc Imaging*. 2023;24(5):e65-e85. https://doi.org/10.1093/ehjci/jead024

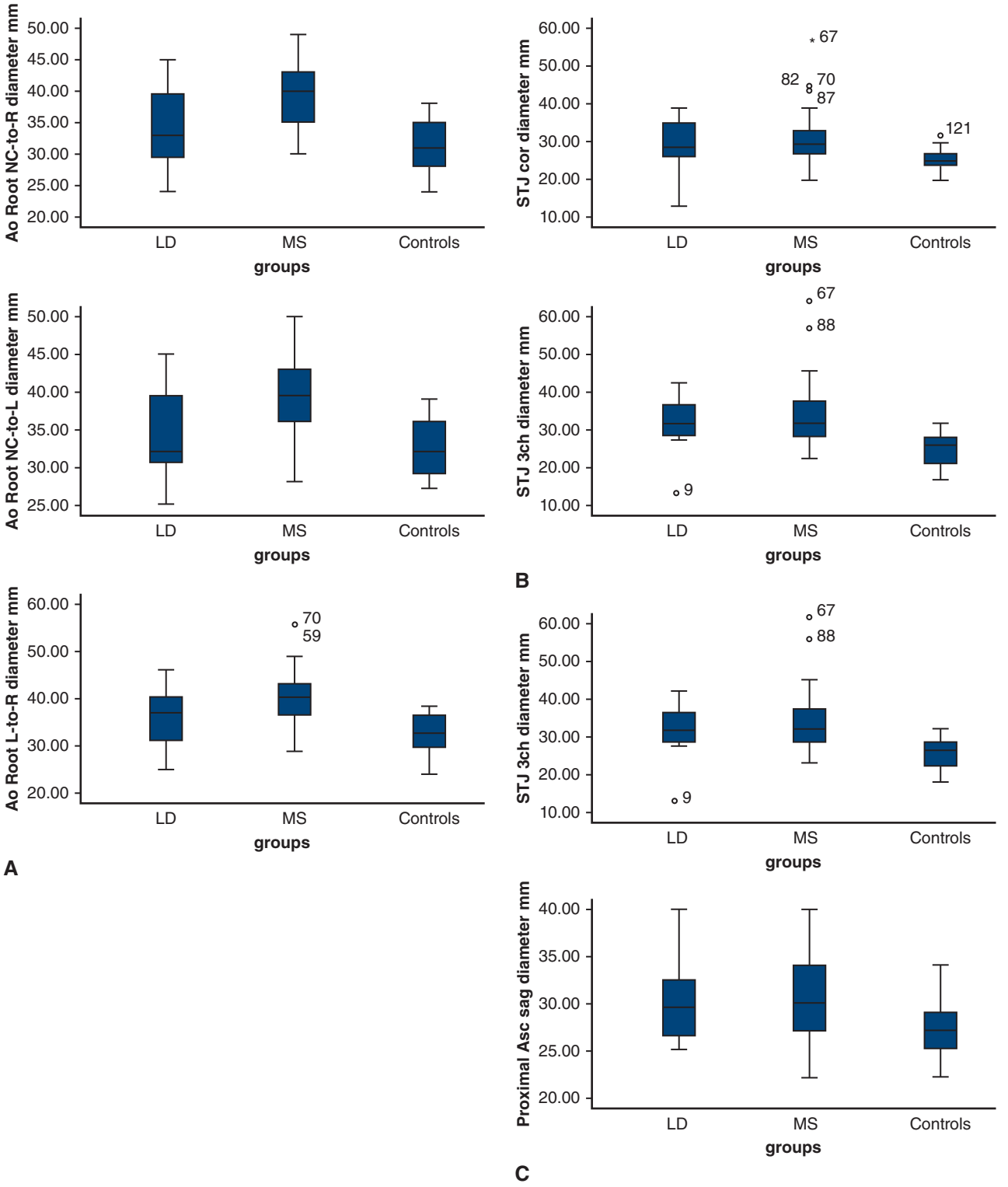

FIGURE E1. Box plot representation of aortic absolute diameters distribution of the whole thoracoabdominal aorta (A-J) in patients with LDS, patients with MFS, and controls. Aortic diameter differences between controls and patients with MFS are greater than aortic diameter differences between controls and patients with LDS. Lower and upper box borders represent 25th and 75th percentiles. The *middle horizontal lines* represent the median. The lower and upper whiskers represent minimum and maximum values of nonoutliers. Extra *dots* (*,°) mark the outliers. *Ao*, Aortic; *NC*, noncoronary; *R*, right coronary sinus; *LD*, Loeys-Dietz; *MS*, Marfan Syndrome; *L*, left coronary sinus; *STJ*, sinotubular junction; *cor*, coronal; *ch*, chambers; *Asc*, ascending aorta; *sag*, sagittal; *Pulm Bif*, pulmonary bifurcation; *SR*, suprarenal; *MT*, middle thoracic; *Diaph*, diaphragmatic; *MFS*, Marfan syndrome.

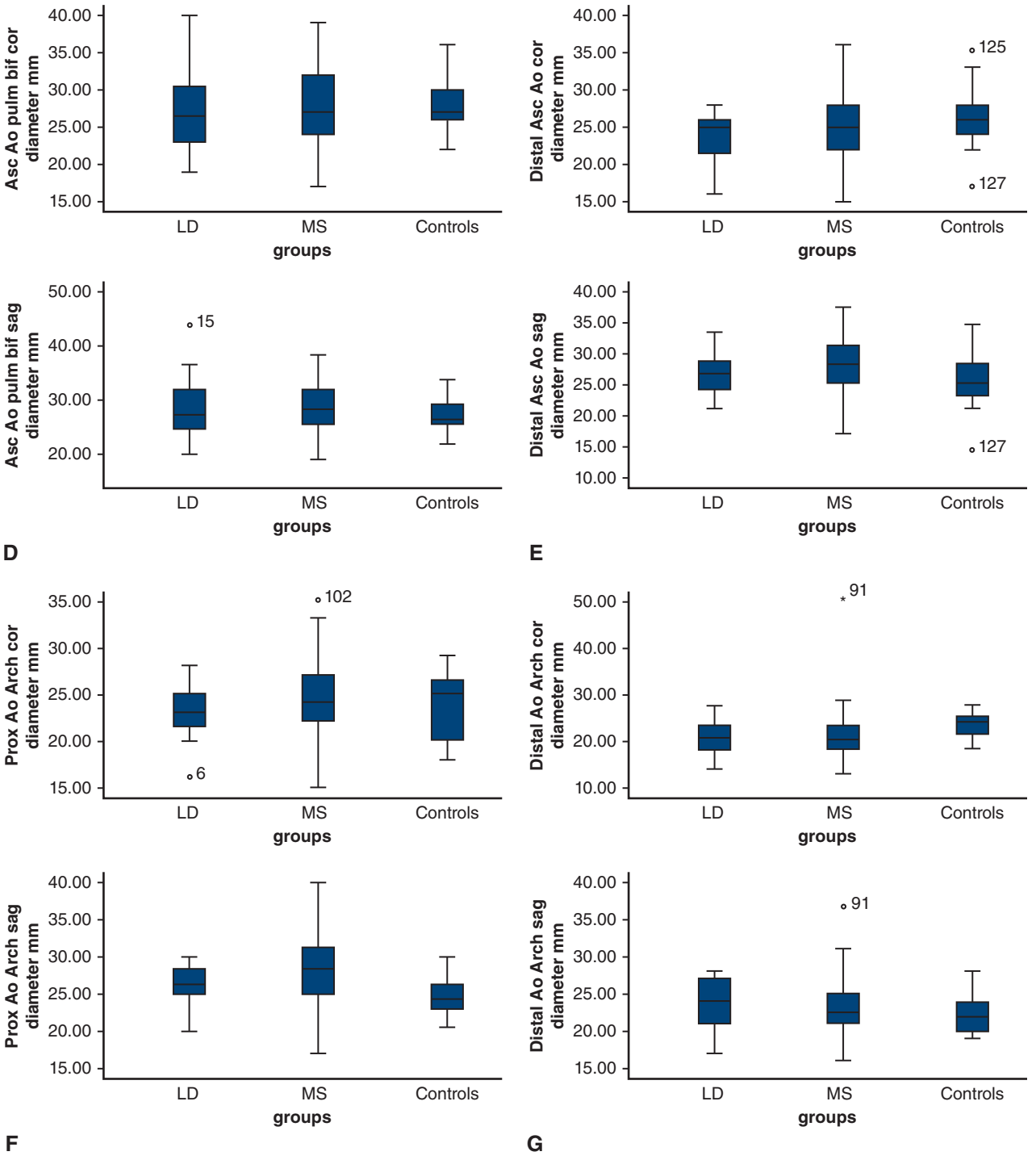

FIGURE E1. Continued.

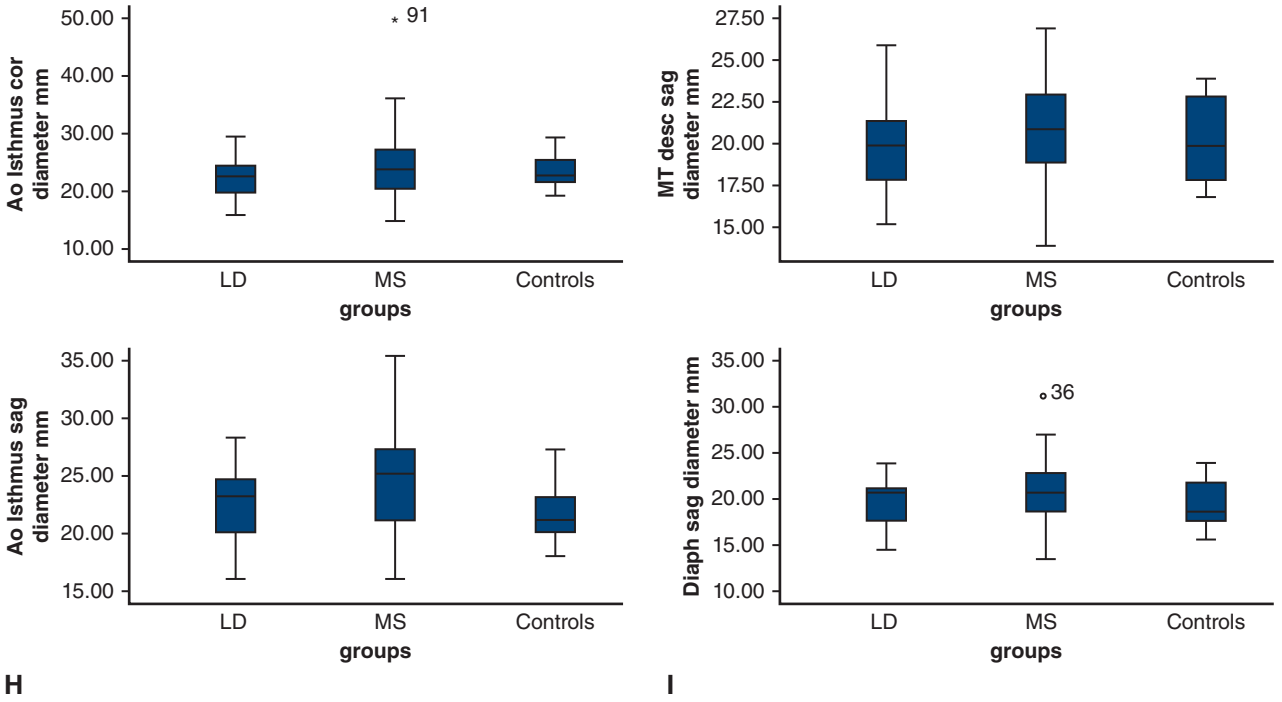

H I

FIGURE E1. Continued.

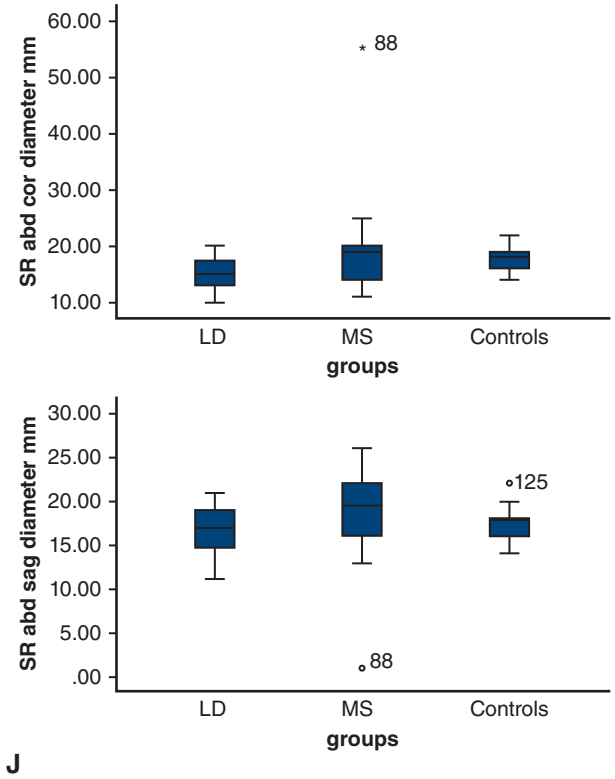

FIGURE E1. Continued.

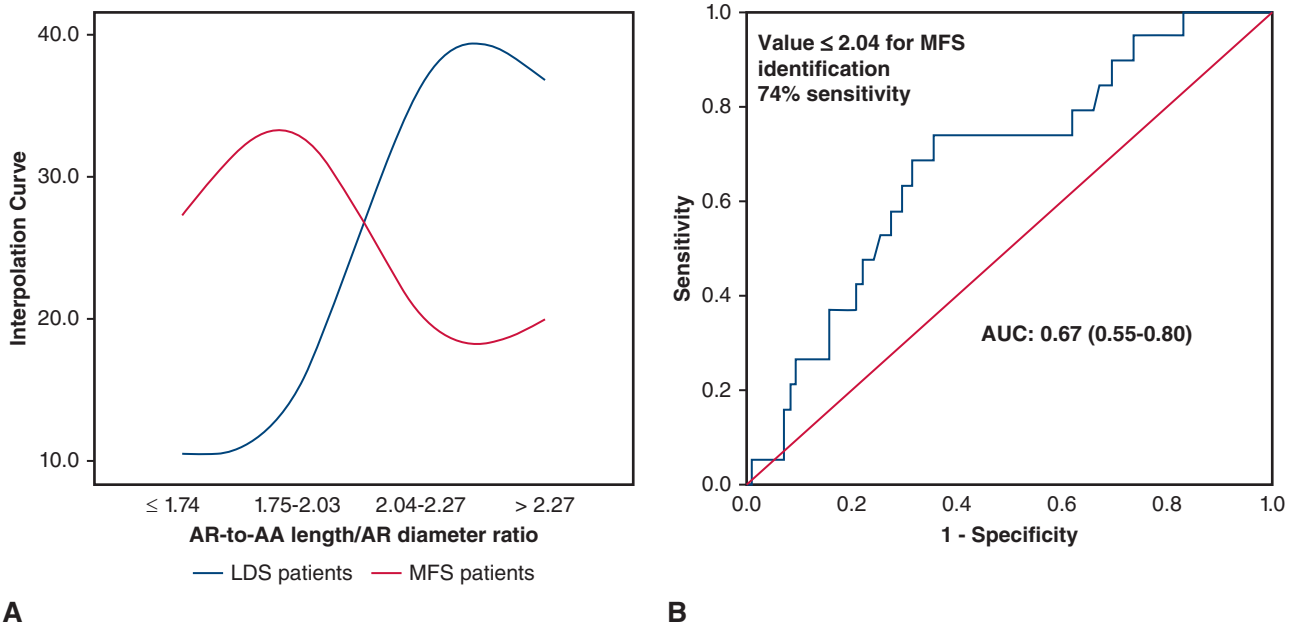

FIGURE E2. Performance of AR-to-AA length/AR diameter ratio for LDS and MFS differentiation. Spline interpolation (A) and ROC curve (B) of AR-to-AA length/AR diameter ratio in LDS and MFS populations. The intersection of spline interpolation curve representing the 2 populations corresponds to the cutoff value; the respective curve position and trend illustrate its discriminating effect, and the ROC curve quantifies its accuracy. *LDS*, Loeys-Dietz syndrome; *MFS*, Marfan syndrome; *AR*, aortic root; *AA*, ascending aorta.

TABLE E1. Comparison of thoracoabdominal aortic diameters (absolute and body surface area indexed) in patients with Loeys-Dietz syndrome, patients with Marfan syndrome, and controls

Aortic segment diameters	LDS* (N = 19)	MFS* (N = 95)	Controls* (N = 20)	*P* (LDS vs MFS)	*P* (LDS vs controls)	*P* (MFS vs controls)
Absolute values						
NC to R	33 (29.2-39.7)	40 (35-43)	31 (28-35.5)	**.001**†	.208	**.000**
NC to L	32 (30.2-39.7)	39.5 (35.75-4)	32 (29-36.5)	**.003**	.433	**.000**
L to R	36.5 (30.2-40.5)	40 (36-43.2)	32 (29-37)	**.005**	.116	**.000**
STJ cor	28.5 (26-35)	29.5 (27-33)	25 (23.5-27)	.471	**.019**	**.000**
STJ 3ch	31 (28-36.2)	32 (29-37)	27 (23-29)	.423	**.001**	**.000**
Proximal AA						
cor	26.5 (24.25-29.75)	28 (25-32)	26 (24.5-29)	.328	.735	.112
sag	29.5 (26.25-32.7)	30 (27-34)	27 (25-29)	.592	**.043**	**.001**
AA pulm bif						
cor	26.5 (22.5-30.7)	27 (24-32)	27 (26-30)	.707	.440	.391
sag	28 (25-33)	29 (26-33.2)	27 (25.5-30)	.664	.380	**.032**
Distal AA						
cor	25 (21.2-26)	25 (22-28.5)	26 (24-28)	.252	.074	.432
sag	26.5 (23.5-28.7)	28 (25-31)	25 (23-28.5)	.204	.423	**.013**
Proximal arch						
cor	23 (21.2-25)	24 (21.75-3)	25 (22.25-26.75)	.336	.149	.652
sag	26 (25-29.2)	28 (25-31.2)	24 (23-26)	.081	**.046**	**.000**
Distal arch						
cor	20.5 (18-23)	20 (18-23)	23.5 (21-24.7)	.626	**.034**	**.001**
sag	24 (21-27)	22.5 (21-25)	22 (20-24.5)	.387	.222	.547
Isthmus						
cor	21 (18.25-22.75)	22 (18.75-2)	21 (20-23.7)	.250	.368	.907
sag	23 (20-24.7)	25 (21-27.2)	21 (19.5-2)	.090	.280	**.004**
MT						
cor	19 (17-20)	19 (18-21)	20 (18-22)	.382	.124	.324
sag	20 (18-21.7)	21 (19-23)	20 (18-23)	.265	.640	.505
Diaphragm						
cor	18.5 (16-20)	19 (16.7-20)	19 (17-21.5)	.477	.370	.668
sag	20 (16.5-20.7)	20 (18-22)	18 (17-21)	.250	.676	**.051**
SR						
cor	15 (13-17.7)	19 (14-20)	18 (16-19)	**.007**	**.009**	.767
sag	17 (14.2-19)	19.5 (16-22)	18 (15.5-18)	**.014**	.643	**.019**
Indexed values						
NC to R	18.52 (16.4-22.8)	21.06 (19.5-22.8)	17.0 (16.4-18.4)	**.041**	.075	**.000**
NC to L	18.67 (16.9-23.3)	21.1 (19.1-22.4)	17.9 (17.1-19.2)	.112	.220	**.000**
L to R	19.94 (17.4-23.2)	21.27 (19.5-23.2)	17.3 (16.4-18.8)	.192	**.015**	**.000**
STJ cor	17.08 (14.8-19.4)	15.78 (14.4-17.2)	13.7 (13.2-14.9)	.302	**.002**	**.000**
STJ 3ch	17.48 (16.1-20.9)	17.23 (15.7-19.5)	14.0 (13.3-14.8)	.417	**.000**	**.000**
Proximal AA						
cor	14.8 (13.8-17.5)	15.26 (13.2-16.8)	14.4 (13.7-15.7)	.839	.481	.362
sag	16.32 (15.1-19.6)	16.35 (14.2-17.9)	14.7 (13.5-16.5)	.327	.010	.011
AA pulm bif						
cor	13.9 (13.2-17.8)	14.92 (12.5-16.3)	15.0 (14.0-16.4)	.345	.646	.256
sag	15.44 (14.3-19.1)	16.04 (13.9-17.5)	14.8 (13.7-15.7)	.350	.104	.126
Distal AA						
cor	13.36 (12.9-14.5)	13.63 (11.9-15.0)	14.0 (13.2-15.7)	.909	.198	.134
sag	15.07 (13.7-16.6)	15.47 (13.2-16.4)	14.2 (12.6-14.8)	.771	.061	.014
Proximal arch						
cor	13.38 (12.-14.2)	13.23 (11.1-14.9)	13.5 (12.6-14.1)	.839	.726	.716
sag	14.98 (13.7-16.6)	15.16 (13.5-17.2)	13.6 (12.8-14.1)	.634	.006	**.002**

(Continued)

TABLE E1. Continued

Aortic segment diameters	LDS* (N = 19)	MFS* (N = 95)	Controls* (N = 20)	*P* (LDS vs MFS)	*P* (LDS vs controls)	*P* (MFS vs controls)
Distal arch						
cor	11.91 (10.5-13.2)	10.65 (9.2-12.4)	12.9 (12.0-13.2)	.079	.308	**.000**
sag	13.43 (12.1-14.3)	12.06 (10.7-13.5)	12.4 (11.5-13.0)	**.026**	.057	.752
Isthmus						
cor	11.6 (10.8-13.4)	11.86 (9.9-13.5)	11.6 (10.65-13.2)	.958	.849	.739
sag	12.86 (11.5-14.3)	12.93 (11.2-14.7)	11.6 (10.8-12.4)	.708	.066	.010
MT						
cor	11.66 (10.1-12.6)	11.09 (9.8-12.1)	11.1 (10.5-12.0)	.363	.443	.028
sag	11.66 (10.1-12.6)	11.09 (9.8-12.1)	11.1 (10.5-12.0)	.345	.646	.646
Diaphragm						
cor	10.06 (9.4-11.8)	9.9 (8.84-11.2)	10.6 (9.6-11.0)	.448	.783	.262
sag	10.6 (9.9-12.3)	10.7 (9.37-11.9)	10.0 (9.4-10.7)	.832	.150	.164
SR						
cor	8.85 (7.4-9.5)	9.6 (8.0-11.3)	9.5 (8.9-10.4)	.055	.009	.962
sag	9.52 (8.4-10.5)	10.5 (8.9-11.6)	9.4 (8.6-10.3)	.061	.759	.027

Larger aortic diameter differences are evident between controls and MFS compared with LDS and controls. AR diameters in LDS and controls are not significantly different. *LDS*, Loeys-Dietz syndrome; *MFS*, Marfan syndrome; *NC*, noncoronary; *R*, right; *L*, left; *STJ*, sinotubular junction; *AA*, ascending aorta; *cor*, coronal; *sag*, sagittal; *Pulm Bif*, pulmonary bifurcation; *MT*, middle thoracic; *SR*, suprarenal; *AR*, aortic root. *Values are median (IQR). †Statistically significant differences are marked by bold numbers.

TABLE E2. Comparison of aortic segments area and tortuosity index between patients with Loeys-Dietz syndrome and patients with Marfan syndrome

	Area (mm^2)*			Tortuosity index*		
Aortic segments	MFS (n = 95)	LDS (n = 19)	*P*	LDS (n = 19)	MFS (n = 95)	*P*
STJ	895 (687-1482)	725 (562-949)	.120	-	-	-
Proximal AA	618 (547-820)	783 (610-910)	.152	-	-	-
PB AA	588 (472-815)	672 (491-836)	.390	-	-	-
Distal AA	538 (431-679)	523 (406-585)	.701	-	-	-
Proximal arch	492 (386-644)	523 (419-585)	.799	1.16 (1.11-1.38)†	1.21 (1.16-1.29)	.425
Distal arch	354 (303-443)	426 (321-511)	.116	-	-	-
Isthmus	407 (297-516)	377 (327-472)	.551	-	-	-
DMTA‡	310 (265-388)	299 (224-378)	.292	1.03 (1.01-1.09)	1.04 (1.01-1.07)	.834
Diaphragmatic	294 (237-367)	270 (204-315)	.141	-	-	-
Suprarenal	267 (174-356)	223 (145-288)	.057	1.05 (1.01-1.10)	1.02 (1.01-1.05)	.169
Subrenal	190 (124-222)	151 (132-242)	.581	1.01 (1.00-1.08)	1.02 (1.00-1.06)	.183
Right iliac artery	67 (47-104)	60 (44-67)	.403	1.03 (1.00-1.2)	1.05 (1.02-1.09)	.177
Left iliac artery	67 (48-95)	63 (36-77)	.571	1.05 (1.01-1.14)	1.05 (1.02-1.11)	.335

MFS, Marfan syndrome; *LDS*, Loeys-Dietz syndrome; *STJ*, sinotubular junction; *AA*, ascending aorta; *PB*, pulmonary bifurcation; *DMTA*, descending middle thoracic aorta; *IQR*, interquartile range. *Values are median (IQR). †Tortuosity was calculated for the combined aortic arch-isthmus segment. ‡Tortuosity index refers to the whole descending thoracic aorta.